Neuropsychologia 147 (2020) 107581

Contents lists available at ScienceDirect

Neuropsychologia

journal homepage: http://www.elsevier.com/locate/neuropsychologia

Intensity- and timing-dependent modulation of motion perception with transcranial magnetic stimulation of visual cortex☆

Olga Lucia Gamboa Arana [a], Hannah Palmer [a], Moritz Dannhauer [a], Connor Hile [a], Sicong Liu [a], Rena Hamdan [a], Alexandra Brito [a], Roberto Cabeza [b,c], Simon W. Davis [c,d], Angel V. Peterchev [a,e,f,g], Marc A. Sommer [b,c,e,h], Lawrence G. Appelbaum [a,c,*]

[a] Department of Psychiatry and Behavioral Sciences, Duke University School of Medicine, USA
[b] Department of Psychology & Neuroscience, Duke University, USA
[c] Center for Cognitive Neuroscience, Duke University, USA
[d] Department of Neurology, Duke University School of Medicine, USA
[e] Department of Biomedical Engineering, Duke University, USA
[f] Department of Electrical & Computer Engineering, Duke University, USA
[g] Department of Neurosurgery, Duke University School of Medicine, USA
[h] Department of Neurobiology, Duke University School of Medicine, USA

ARTICLE INFO

Keywords:
Transcranial magnetic stimulation
TMS
Visual motion
Visual evoked potential
TMS Evoked potential
Motion sensitive cortex

ABSTRACT

Despite the widespread use of transcranial magnetic stimulation (TMS) in research and clinical care, the dose–response relations and neurophysiological correlates of modulatory effects remain relatively unexplored. To fill this gap, we studied modulation of visual processing as a function of TMS parameters. Our approach combined electroencephalography (EEG) with application of single pulse TMS to visual cortex as participants performed a motion perception task. During each participants' first visit, motion coherence thresholds, 64-channel visual evoked potentials (VEPs), and TMS resting motor thresholds (RMT) were measured. In second and third visits, single pulse TMS was delivered at one of two latencies, either 30 ms before the onset of motion or at the onset latency of the N2 VEP component derived from the first session. TMS was delivered at 0%, 80%, 100%, or 120% of RMT over the site of N2 peak activity, or at 120% over vertex. Behavioral results demonstrated a significant main effect of TMS timing on accuracy, with better performance when TMS was applied at the N2-Onset timing versus Pre-Onset, as well as a significant interaction, indicating that 80% intensity produced higher accuracy than other conditions at the N2-Onset. TMS effects on the P3 VEP showed reduced amplitudes in the 80% Pre-Onset condition, an increase for the 120% N2-Onset condition, and monotonic amplitude scaling with stimulation intensity. The N2 component was not affected by TMS. These findings reveal the influence of TMS intensity and timing on visual perception and electrophysiological responses, with optimal facilitation at stimulation intensities below RMT.

1. Introduction

Transcranial magnetic stimulation (TMS) has become a valuable treatment option for a host of psychiatric and neurological disorders and a useful tool in the study of the psychophysiology of human cognition. The underlying neural mechanisms that lead to these effects, however, are relatively poorly understood. While a rich literature of studies now offer characterization of transient induced, and plastic long-term, effects of TMS in the motor system (Hallett et al., 2017; Pascual-Leone et al., 1995), systematic dose–response characterization in the visual system, including evaluation of the intensity and timing of stimulation effects, is limited.

TMS to the visual system can yield non-retinal perceptions, referred to as "phosphenes" for static flashes or "mophenes" if perceptual motion

☆ **Disclosures:** A.V.P. is inventor on patents and patent applications on TMS technology. Related to TMS, in the past 3 years he has received patent royalties from Rogue Research; research and travel support, consulting fees, and equipment donations from Tal Medical/Neurex Therapeutics; patent application and research support from Magstim; equipment loans and hardware donations from MagVenture; as well as consulting fees from Neuronetics.

* Corresponding author. 400 Trent Dr. Box 3620, Durham, NC, 27710, Duke University School of Medicine, Durham, USA.
E-mail address: greg@duke.edu (L.G. Appelbaum).

https://doi.org/10.1016/j.neuropsychologia.2020.107581
Received 3 June 2020; Received in revised form 23 July 2020; Accepted 4 August 2020
Available online 12 August 2020
0028-3932/© 2020 Elsevier Ltd. All rights reserved.

is induced (Pascual-Leone and Walsh, 2001; Schaeffner and Welchman, 2017), as well as modulation of perception from retinal input (de Graaf et al., 2014). Notably, single-pulse TMS (spTMS) and paired-pulse TMS (ppTMS) of the visual cortex have been widely reported to induce changes in the perception of visual motion (Bosco et al., 2008; Grasso et al., 2018; Laycock et al., 2007; Silvanto et al., 2005; Vetter et al., 2015). Across a number of studies, TMS to motion sensitive cortex has been shown to influence speed perception (Matthews et al., 2001) and direction sensitivity (Campana et al., 2002), as well as perception of biological motion (Mather et al., 2016). Despite this accumulation of literature, the relationship between the reported physiological response and the degree of behavioral engagement across these studies is highly variable, and the links between TMS parameters and their neurophysiological effects have yet to be established.

Studies of motion perception are particularly well-suited for exploring mechanisms of TMS due to the superficial location of motion sensitive cortex and its well-characterized spatiotemporal progression of electroencephalographic (EEG) activation described by the P1/N2/P3 Visual Evoked Potential (VEP) complex. In this progression, it is regarded that the initial P1 component reflects pattern-related activity of the parvo-cellular subsystem, while the subsequent N2 component has been associated with motion perceptual sensitivity (Bach and Ullrich, 1997; Kuba et al., 2007; Martin et al., 2010) and is localized to the direction-selective area V5 of the extra-striate visual cortex (Pazo-Álvarez et al., 2004). In lateralized visual attention tasks, this response has been characterized as pre-attentive in the early (<200 ms) phase, and specific to spatial attention after about 200 ms, as observed in the widely-reported N2pc component (Clark, Appelbaum, van den Berg, Mitroff and Woldorff, 2015; Luck and Hillyard, 1990). Lastly, in tasks where response selection is made on motion stimuli, a central positive P3 component is frequently observed around 300 ms (Kuba et al., 1998; Kubová et al., 2002) that is thought to reflect attentional allocation to the stimuli (Duncan-Johnson and Donchin, 1982). While other thalamo-cortical pathways also contribute to visual motion perception, these VEPs offer specific testable neural markers that can be characterized to infer dose–response properties of TMS.

The present study builds on these two bodies of literature, TMS modulation of motion perception and motion-induced VEPs, to characterize dose–response functions of spTMS in the visual cortex. Our approach was to measure concurrent TMS-EEG during an individually calibrated, dot-motion, direction-discrimination task, previously developed by our group to test ppTMS effects (Gamboa et al., 2020). For this purpose, we used a three-visit study design consisting of an initial dose-finding session to derive individualized motion coherence thresholds and stimulation parameters based on the onset of the N2 VEP component ("N2-Onset"), followed by two dose-testing sessions during which spTMS was delivered according to the spatial, temporal, and intensity parameters derived from the first session. During the dose-testing sessions, spTMS was delivered at one of two different timings, either 30 ms before the onset of motion ("Pre-Onset", based on the observation that TMS to V5 around this latency can disrupt motion perception (Beckers and Homberg, 1992; Beckers and Zeki, 1995; D'Alfonso et al., 2002; Sack et al., 2006), or at the N2-Onset latency for each participant measured during the first session. During each of these two sessions, participants performed eight blocks of trials with intermixed pulse intensities at 0%, 80%, 100%, and 120% of resting motor threshold (RMT) delivered over the hotspot of the N2-Onset component, as well as two separate blocks of trials at 120% RMT delivered at the vertex of the head, therefore serving as a control location. As such, this study tested the effects of spTMS over intensities that have previously been reported to induce facilitatory and inhibitory perceptual effects (Luber et al., 2020; Silvanto et al., 2017), but at different timings relative to the motion onset and at different cortical targets. In addition, this approach includes use of two reference conditions, no-stimulation trials with 0% RMT intensity and 120% RMT delivered to the vertex, for experimental control.

The overall goal of the study was therefore to map the behavioral and evoked EEG dose–response functions within the constructs of this individualized spatiotemporal targeting. We had two complimentary hypotheses on the capacity of intensity-dependent TMS to affect changes in brain and behavior. Our first hypothesis was that spTMS delivered at the precise onset of the N2 component disrupts motion processes in the brain more than TMS simply delivered at the onset of motion, leading to monotonically increasing effects across different stimulation intensities due to the putative inhibitory effects of spTMS and state-dependency induced by the motion task. Our second hypothesis was that such precisely timed TMS would have significant effects on subsequent VEPs, such that while we did not expect to observe significant changes in the Pre-Onset condition, but we did anticipate reduced amplitude of the P3 component as a manifestation of processing interruptions from stimulation at the onset of the N2 response. We expected that the results of testing these hypotheses would contribute to a coherent neurocognitive framework in which to interpret the intensity-based responses to temporally- and spatially-precise TMS applications.

2. Methods

2.1. Participants

Twenty-four healthy volunteers (15 females, M_{age} = 23, SD_{age} = 2.55) enrolled in this 3-visit study. All participants were self-reported right-handed, had normal or corrected-to-normal vision, and were screened for contraindications to TMS (Rossi et al., 2009). Exclusion criteria included a history of neurological or psychiatric disease and/or use of psychoactive medication, a personal history of head trauma with loss of consciousness or family history of epilepsy or seizures. Informed consent was obtained for each participant after explanation of study requirements under an experimental protocol approved by the Duke University Institutional Review Board (Pro00082433). Participants were compensated $20 per hour for their time.

2.2. Experimental design and equipment

This study consisted of three sessions, each lasting 2–3 h, performed on separate visits within a three-week span. Twenty-one participants completed the first dose-finding session, with 18 and 17 completers for the Pre-Onset and N2-Onset sessions, respectively. In total, 15 of the participants completed all three sessions, while the remaining participants only completed one or two of the sessions due to scheduling conflicts, illness, or equipment difficulty.

All stimuli were generated using Matlab (Mathworks, Natick, MA, USA) and the Psychtoolbox extension (Brainard, 1997) and presented on a 21-inch monitor with 60 Hz refresh rate and 1920 × 1050 resolution. EEG was acquired on all three visits using a 64-channel actiCHamp EEG system (BrainProducts, Munich, Deutschland) and TMS compatible actiCAP with slim active electrodes arranged according to an equidistant montage. The EEG signal was digitized at a sampling rate of 5 kHz and referenced utilizing the FCz electrode according to the 10–20 placement system. TMS was delivered using a MagPro R30 stimulator connected to a Cool-B65 figure-of-eight coil (MagVenture, Farum, Denmark). An Arduino board was employed to control the triggering of the TMS device relative to the stimulus onset, with a temporal precision of approximately 1 ms, based on TMS device output and a Photo Sensor (BrainProducts, Munich, Germany) detecting stimulus onset.

A Brainsight (Rogue Research, Canada) frameless stereotactic neuronavigation system was used to monitor TMS coil position on the participant's head so that the stimulation location was kept as constant as possible. For this, coil trackers were attached to the coil and the participant's head, which was registered to the Montreal Neurological Institute standard brain atlas using anatomical landmarks. A coil holder and a chin rest were also used to maintain stable coil and head positioning. In addition, a spacer was used to minimize contact with the

electrodes and associated EEG artifacts (Ruddy et al., 2018), while a thin foam sheet (~1 mm) was added to minimize bone conduction of the TMS sound and scalp sensations caused by mechanical vibration of the coil. Participants wore earplugs for hearing protection and mitigation of auditory activation by the TMS pulse clicks. Two experimenters were always present in the room, to maintain coil positioning and supervise EEG data quality.

2.2.1. Session 1: dose-finding

During the first session, eligibility was assessed and consent was obtained. Following this, the 64-channel EEG cap was fitted to the participant's head and after applying gel the RMT was acquired, taking about 15 min according to the procedures described below. This allowed for estimations of stimulation intensity calculation according to RMT with equivalent distancing between the head and coil as used in the dose-testing sessions. Participants then performed 20 min of practice of the motion task (Fig. 1A) while EEG impedances were being adjusted and recordings were prepared. After obtaining clean EEG signals, with impedances below 5 kΩ, the participant completed four, 8-min runs of the motion discrimination task.

2.3. Resting motor threshold (RMT)

RMT was defined as the lowest intensity required to elicit a motor evoked potential (MEP) of 50 μV peak-to-peak when the muscle was at rest (Conforto, Z'Graggen, Kohl, Rösler and Kaelin-Lang, 2004). Surface electromyogram was recorded from the right first dorsal interosseous muscle by using disposable electrodes (Covidien/Kendall, 133 Foam EMG Electrodes, Mansfield, USA) in a belly tendon montage. After establishing a reliable stimulation site according to the visual-twitch method, RMT was determined by a probabilistic threshold-hunting method using the Motor Threshold Assessment Tool software (http://www.clinicalresearcher.org/software.html).

2.4. Motion direction discrimination task and visual evoked potential

A common dot motion discrimination task was employed across all sessions of this experiment. In the first dose-finding session of the study, the coherence of dot motion varied randomly from trial to trial, allowing for the estimation of each individual's threshold coherence value, which was then fixed to this level for each participant in sessions 2 and 3.

In this task, each trial initiated with a white fixation cross appearing for 500 ms, after which two fields of static white dots appear within 12.6° circular windows centered 7.6° to the left and right of fixation. These dots remained static for a variable duration between 400 and 800 ms, after which the dots moved briefly for 75 ms at a speed of 15.5 deg/s. The dots in the left field moved incoherently in random directions while the dots in the right field contained some level of directional coherence, which was randomly selected to be 0, 20, 40, 60, 80, or 100% on each trial. Following the motion, participants had 2 s to indicate with a button press if the direction of motion was to the left or upwards. After each answer, feedback was provided with a green fixation cross for correct responses and red for incorrect responses that was presented for 1 s. The viewing distance (eye-to-screen center) for each participant was kept constant at approximately 56 cm and all the participants were instructed to perform the task as accurately as possible within the 2 s allotted time.

At the end of the first session, a generalized linear model was applied to fit a sigmoid function to the assigned (+1/−1 due to dot motion direction) trial coherences and correct/incorrect responses to determine the 75% accuracy point on the coherence psychometric curve. If 75% accuracy could not be achieved, then 100% dot motion coherence was used. As described in greater detail in section 2.3.2, concurrent EEG was collected and analyzed for VEP results. As described in Section 3.1, these analyses led to characterization of an N2 onset latency and location that was used for dosing in Sessions 2 and 3.

2.4.1. Sessions 2 and 3: dose-testing

During Sessions 2 and 3, participants performed the same motion

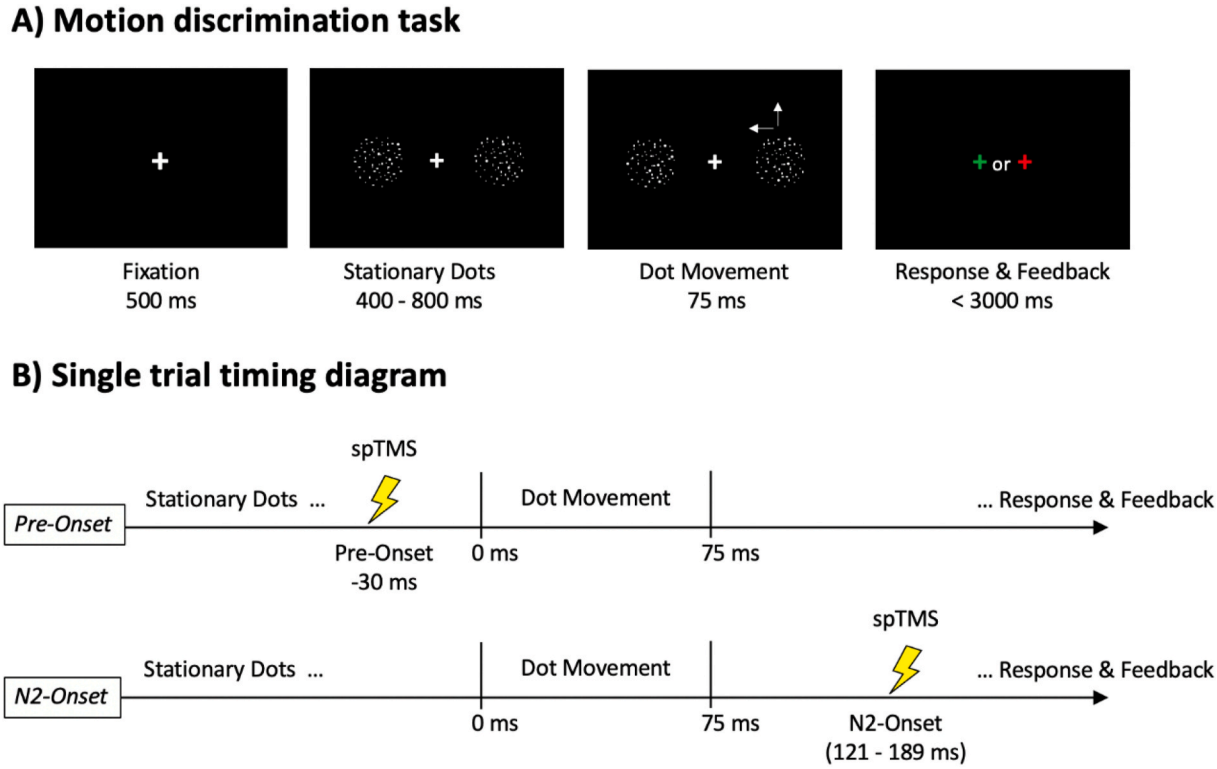

Fig. 1. Schematic illustrations of A) motion direction discrimination task showing four example frames and the duration of each sequence, and B) schematic of TMS (lightning bolts) relative to dot motion for the Pre-Onset and N2-Onset conditions.

task with dot stimuli presented only at the threshold coherence level determined from Session 1. These sessions differed only in the latency at which TMS was applied relative to the onset of the motion on each trial. As illustrated in Fig. 1B, biphasic spTMS was applied either 30 ms before the onset of motion (Pre-Onset) or at the onset latency of the N2 component (N2-Onset) derived from Session 1. The V5 target was defined as the topographic location showing the most robust N2 response identified from the current source density (CSD) maps corresponding to the N2 sink topography (see right column of Table 1). Consistent with what is known about motion sensitive cortex (Silvanto et al., 2005), this topographic localization pointed to electrodes over the left occipital cortex, as the regions (referred to here as V5) displaying maximal activity, and this location was targeted with TMS. The center of the coil was placed tangentially to this stimulation site with the handle pointing towards the right hemisphere.

On both of these sessions the procedures were identical and began with the participant practicing the motion task as the cap was placed, gel applied, and impedances checked and adjusted. After a clean EEG signal was achieved with impedances below 5 kΩ, the participant began eight 4-min blocks of 56 trials each while receiving spTMS. In six of the eight blocks, TMS was delivered to the V5 target channel at intensities of 0%, 80%, 100% or 120% RMT, controlled remotely using a customized function from MAGIC Matlab toolbox (Saatlou et al., 2018). These intensities were delivered for all trials within a block and changed according to a random sequence created for each block at the beginning of the session. The two remaining blocks were assigned to stimulation of the vertex during task performance at 120% of RMT (112 trials). Stimulation over vertex was performed as a control condition. Vertex was defined as the scalp location corresponding to Cz in the 10–20 system. The coil handle was parallel to the midline pointing backwards. Two blocks of stimulation delivered over vertex were randomly distributed throughout the eight total blocks, as determined by an ordering calculation done at the second and the third session, respectively.

Table 1
Experimental parameters collected in Session 1. Stimulation intensity at RMT, motion coherence thresholds, stimulation times and closest stimulated channels (See Fig. 1A for locations) for the closest EEG electrodes relative to the position of stimulation in Sessions 2 and 3. The coil was positioned approximately over the center of mass surrounding these electrodes, based on the N2 topography in visit 1, as guided by BrainSight neuronavigation. Asterisk (*) indicates subjects with complete data that were included in the rmANOVA described in Section 3.2.

Subject Number	RMT (% MSO)	Percent Dot Coherence	Stimulation Timing (ms)	Closest Stimulated Channels
S1*	54	37	184	18, 20
S2*	57	74	160	20, 24, 21
S3*	81	100	161	20, 24, 25
S4*	57	75	143	23, 24
S5*	83	92	170	20, 24
S6	55	100	119	25, 51
S7	83	100	156	21, 24
S8	71	100	166	24,25
S9*	64	100	129	20, 21, 24, 25
S10*	64	100	189	20, 24, 25
S11*	62	82	151	24, 25
S12	65	100	158	20, 25
S13	82	100	121	20
S14	55	100	152	20, 24
S15*	80	100	153	24, 20, 21
S16	58	50	148	25, 20, 24
S17*	52	100	141	25, 20,24
S18*	50	76	163	20, 21, 24
S19*	63	100	125	25, 20
S20*	77	100	174	24, 23, 21
S21*	44	84	148	24, 25, 20

2.5. Analyses

2.5.1. Behavioral data analyses

One-way ANOVA were performed to evaluate the effect of dot coherence in the initial dose-finding session. To evaluate experimental effects in the dose-testing sessions changes in accuracy were examined by a repeated measure ANOVA (rmANOVA) with factors Stimulation Condition (0%, 80%, 100%, and 120% RMT at V5 and 120% RMT at vertex) and TMS Timing (Pre-Onset and N2-Onset). Additionally, to provide a more sensitive assessment of the effects of TMS intensity, 2×4 rmANOVA was performed, on the "normalized" accuracy data, calculated by subtracting the 0% RMT condition from each of the other conditions. Because the 0% condition displays the same visual stimuli, but no TMS pulse or associated sounds and sensation, this subtraction creates an effective baseline to account for non-TMS related activity. Post hoc pairwise comparisons were tested using Tukey's HSD method. A Shapiro-Wilks test was used to verify the assumption of normality while Mauchly's test evaluated the assumption of sphericity. A Greenhouse-Geisser correction was adopted when the sphericity assumption was violated. Statistical tests were performed using SPSS 25.0 (SPSS Inc, Chicago) and p values $\leq .05$ were considered statistically significant.

2.5.2. EEG data processing and analysis

EEG data were preprocessed and analyzed offline using Brain Vision Analyzer (Brain Products, Inc.) and Matlab (Mathworks, Natick, MA, USA), in a manner modeled after Rogasch et al. (2014). Data were down sampled to 1000 Hz, TMS pulses were removed via linear interpolation spanning from 10 ms before to 25 ms after the pulse. Before applying Independent Component Analysis (ICA) to identify and discard artifactual components such as eye blinks and muscle activity, the EEG signal was bandpass filtered using a zero-phase shift Butterworth filter (0.1–45 Hz) and visually inspected to remove contamination. ICA-based artifact removal was then performed, leading to an average of 10.4 removed components per participant, with no significant difference in the number of components removed across the TMS Timing sessions. Bad electrodes were interpolated before segmentation and baseline correction was performed from −250 to −50 ms for Pre-Onset and −200 to 0 ms for the N2-Onset averages. The final analyzed segments from −200 to 1000 ms were re-referenced to the common average across all channels.

VEPs for both the Pre-Onset and N2-Onset sessions were calculated by averaging artifact–removed trials in each channel. This led to an average of 78 trials per condition and per participant when stimulating at V5, and 103 trials per participant in the vertex stimulation condition. In order to investigate the electrophysiological correlates of visual motion perception, VEP analyses focused on mean activity in two multichannel, regions-of-interest. As shown in Fig. 2D, the V5 ROI comprised the channels 20, 21, 24 and 25, which surrounded the site of stimulation for all subjects. The Central Parietal (CP) ROI consisted of channels 1, 4, 18, 19, 33 and 34, centered over midline parietal cortex, in alignment with previously reported visual motion P3 effects (Kuba et al., 1998; Kubová et al., 2002). Because of the biphasic morphology of the N2 component in this study (See Fig. 2B) and because stimulation in the N2-Onset timing disrupted the first phase of this component, the N2 was examined separately in an early (130–200 ms) and late (230–340 ms) latency window. P3 amplitude was averaged between 250 and 550 ms.

Data from two participants were discarded from the final dose-testing analyses because of high levels of (predominantly blink) ocular artifacts in the N2-Onset sessions. As such, the final analyzed sample consisted of 18 participants with clean Pre-Onset data and 15 participants with clean N2-Onset data. Fourteen of these participants completed both Session 2 and 3 and were included in the rmANOVA (see section 3.2).

In order to focus analyses on the electrophysiological dose–response produced by different intensities, the following analyses compared the

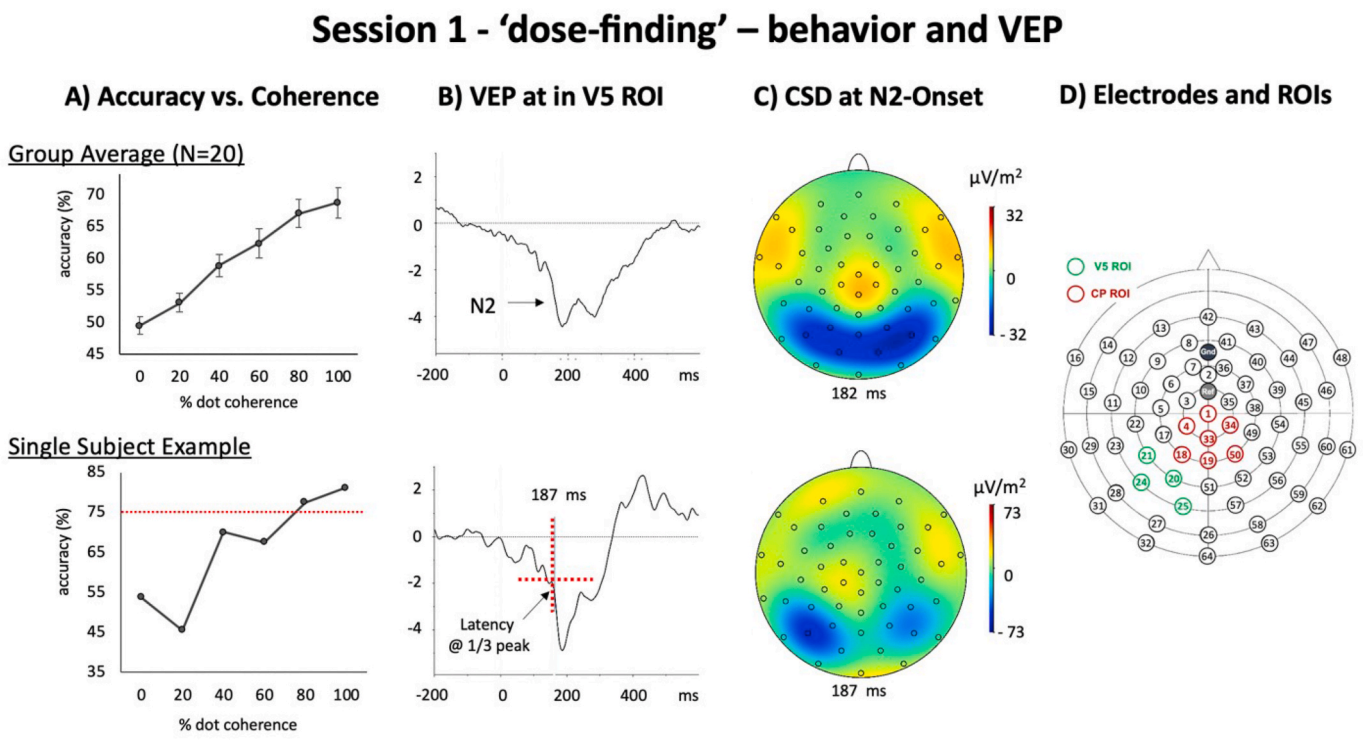

Fig. 2. Behavior and VEP results from Session 1 shown on top for the 20-participant group average and on the bottom for a representative subject. A) Coherence versus accuracy plots. B) VEP to motion onset for correctly reported trials at V5 ROI shows characteristic N2 component. C) Current source density topographic map at calculated N2-Onset. D) Electrode map of 64-channel EEG with V5 ROI (green) and Central Parietal ROI (CP; red). Vertex is channel 1. (For interpretation of the references to color in this figure legend, the reader is referred to the Web version of this article.)

normalized, averaged component amplitudes, subtracting the 0% (no stimulation) condition from each of the other conditions. These analyses were performed separately for the Session 2 and 3, allowing comparisons of components that would be obscured due to the different timing of the TMS pulse. For the Pre-Onset Timing, analyses addressed the early N2, late N2, and P3 components. In the N2-Onset Timing, analyses addressed the late N2 and P3 components. In addition, see **Supplement 1** for description of P1 component and reference sample.

3. Results

3.1. Session 1: dose-finding

3.1.1. RMT results

RMT was successfully derived for all participants through convergence of the adaptive Parameter Estimation by Sequential Testing (PEST) procedure (Borckardt et al., 2006). On average 63.6% of Maximum Stimulator Output (MSO) was required to induce the target EMG response at RMT with a range of 44%–83%, as reported in Table 1.

3.1.2. Accuracy and VEP results

As illustrated in Fig. 2A, participants performed the task at chance in trials that had no coherent movement (0%), with a monotonic increase in accuracy for higher coherence stimuli. One-way ANOVA confirmed a main effect of Percent Dot Coherence (F [2.869,60.249] = 30.472, $p < .001$, $\eta^2 = 0.592$) with an average dot coherence of 91.7% [range 34%–100%] at threshold.

VEPs are time locked to the onset of motion showed a waveform morphology (Fig. 2B and C) dominated by a bilateral negative posterior distribution peaking around 200 ms, which is followed by a positive CP deflection around 300 ms suggesting a N2/P3 ERP complex (Bach and Ullrich, 1997; Kuba et al., 2007; Martin et al., 2010). The N2 component was found in all individual participant's and used to derive the N2-Onset stimulation timing and location. VEPs were processed to calculate the latency at 1/3 max amplitude of the N2 component at its peak location, as it is common in event-related potential studies (Luck, 2014). These locations were consistently located at left occipital channels (20, 21, 24, and 25), which is depicted by the green labels in Fig. 2D. Similar to previous studies using near-threshold motion onset (Kuba et al., 2007; Martin et al., 2010), the VEP did not show a P1 component (Bach and Ullrich, 1997; Kuba et al., 2007; Martin et al., 2010). The P1 response has been previously described as a pattern-sensitive parvocellular--driven component, which may have been absent here due to the 500 ms separation of the dot appearance and motion onset in this task (see **Supplement 1** for more information).

3.2. Dose-testing: behavioral results

Using performance accuracy data from the 14 participants who completed both experimental sessions, the 2 (Stimulation Timing) × 5 (Stimulation Condition) rmANOVA revealed a main effect of Stimulation Timing (F [1,13] = 5.754, $p = .032$, $\eta^2 = 0.307$) with higher accuracy for N2–Onset relative to Pre–Onset (see Fig. 3A). In addition, the Stimulation Timing by Stimulation Condition interaction was significant (F [4,52] = 3.313, $p = .017$, $\eta^2 = 0.203$). Pairwise comparison results demonstrated that, when the stimulation was delivered at the timing of N2-onset, the condition of 80% at V5 led to higher response accuracy than 120% at V5 and 120% at Vertex ($ps \leq .042$).

Results from rmANOVA performed on the normalized behavioral accuracy, shown in Fig. 3B, demonstrate non-significant main effects of Stimulation Timing ($p = .944$) and Stimulation Condition ($p = .360$), but show a significant interaction between these factors (F [3,39] = 4.073, $p = .013$, $\eta^2 = 0.239$). Pairwise comparison results showed that, when the stimulation was delivered at the timing of N2-Onset, the 80% at V5 condition led to higher response accuracy than 120% intensity at both V5 and Vertex locations ($ps \leq .046$).

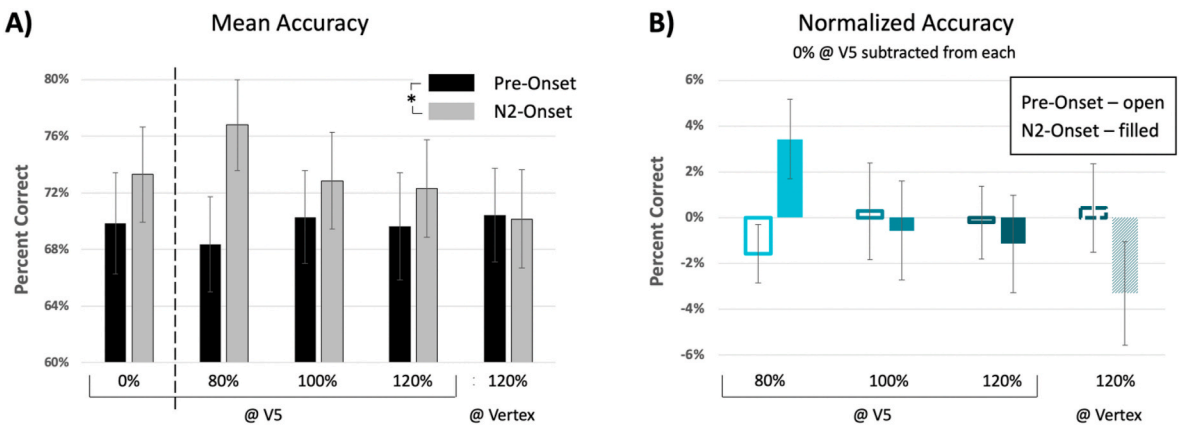

Fig. 3. A) Mean accuracy and standard errors for the five stimulation conditions, for the Pre-Onset (black) and N2-Onset (grey) Stimulation Timings. ANOVA showed significantly higher accuracy for N2-Onset and a significant interaction with higher accuracy at 80% intensity. B) Normalized mean accuracy for each Stimulation Condition and Stimulation Timing minus the 0% condition, shows a significant interaction. Different shades indicate different intensity conditions with lighter colors indicating lower intensities. (For interpretation of the references to color in this figure legend, the reader is referred to the Web version of this article.)

3.3. Dose-testing: EEG results

3.3.1. Pre-Onset stimulation timing

Similar to the behavioral null results ($p = .90$), one-way ANOVA results showed that N2 VEP amplitudes (i.e., early and late N2 responses in the V5 ROI) did not differ across the levels of Stimulation Condition ($p \geq .314$). In contrast, significant differences of P3 VEP amplitude were observed across the levels of Stimulation Condition (F [2.222,37.780] = 4.697, $p = .013$, $\eta^2 = 0.216$). Pairwise comparison results showed that, as displayed in Fig. 4A, mean P3 amplitude for the normalized 80% at V5 condition was significantly smaller than those of all the other stimulation conditions (p values $\leq .014$). To further explore the relationship between behavioral accuracy and VEP changes, Pearson correlations were determined between each of the three normalized VEP amplitudes (i.e., early N2, late N2, and P3) and the normalized response accuracy across all 18 participants. None of the correlation estimates reached statistical significance with corrected alpha level (i.e., 0.05/3 = 0.017).

3.3.2. N2-Onset Timing

One-way ANOVA performed on the four normalized behavioral

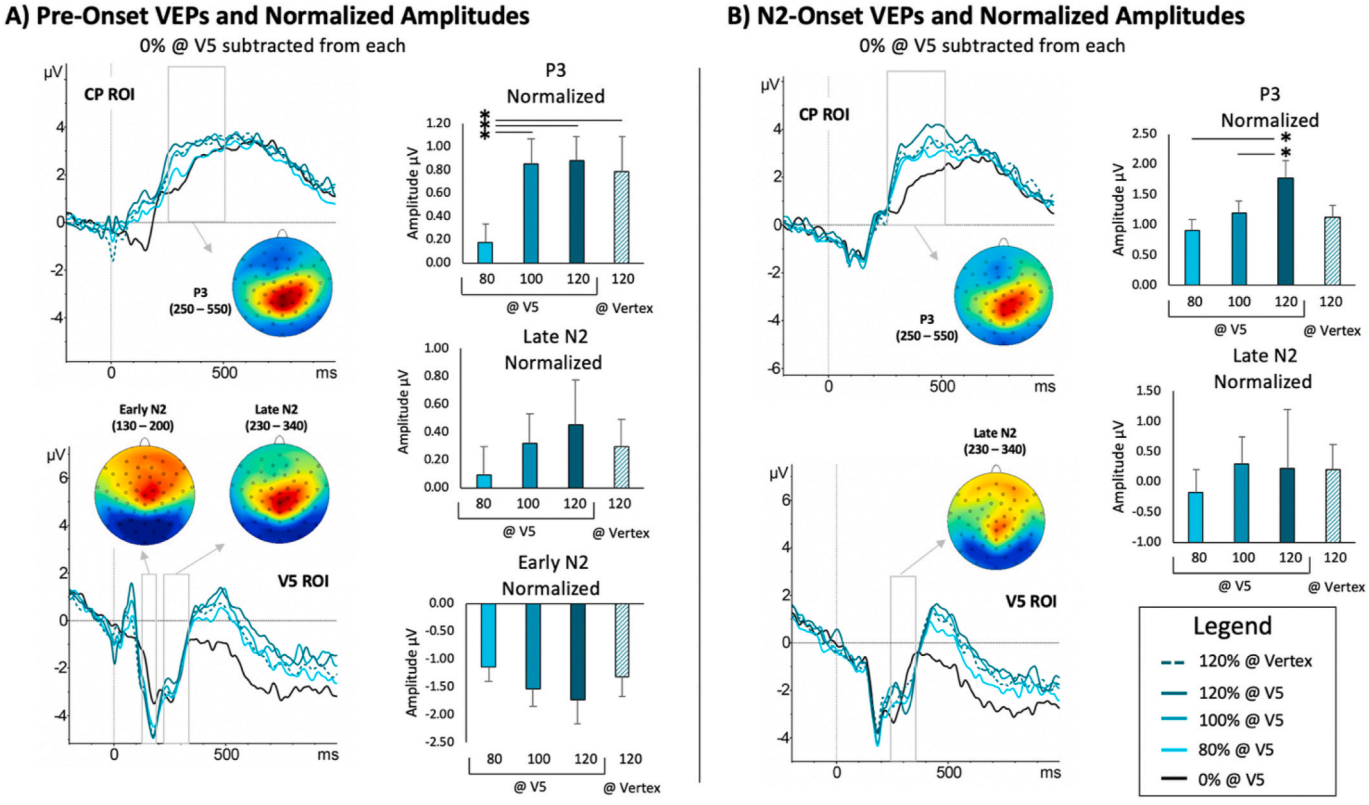

Fig. 4. A) Pre-Onset VEPs, time-locked to the start of motion and shown for the CP (top) and V5 (bottom) ROIs for each of the five Stimulation Conditions (legend in bottom right). CSD topographies for the early N2, late N2 and P3 components are shown in relation to the grey boxes highlighting the latencies that are considered. Bar graphs represent the normalized (subtracting the condition of 0% at V5) mean amplitudes for each Stimulation Condition and Component. B) N2-Onset VEPs, topographies and normalized amplitudes in the same format as panel A, but without the early N2 component, which is obscured by TMS artifact.

accuracy scores, revealed significant differences among stimulation conditions (F [3,42] = 4.794, p = .006, η^2 = 0.255), with higher accuracy for the 80% RMT condition relative to all the other conditions (p *values* ≤ .032), confirming the behavioral effect in this sub-sample of data.

One-way ANOVA results on the late N2 amplitude for the V5 ROI and the P3 amplitude in the CP ROI[1] revealed a significant main effect of Stimulus Condition on the P3 amplitude (F [3,42] = 4.475, p = .008, η^2 = 0.242), but not on the amplitude of the late N2 component (p = .711). Pairwise comparisons indicated that the 120% at V5 condition resulted in higher mean amplitude than the 80% (p = .003) and 100% (p = .019) conditions, as illustrated in Fig. 4B. Pearson correlation coefficients between the individual subject normalized VEP amplitudes and normalized response accuracies were not significant for either the late N2 or P3 components.

4. Discussion

The current study investigated task-relevant dose–response functions of single pulse TMS by examining the influence of stimulation timing and intensity on electrophysiological and behavioral responses. Here, single pulse TMS was applied at two latencies relative to the onset of psychometrically calibrated, near-threshold, motion stimuli to assess the behavioral and electrophysiological changes due to TMS. It was hypothesized that stimulation would lead to greater behavioral disruption in motion direction discrimination and larger VEP effects on the P3 component when stimulated at the onset of the N2 component given the critical links between this component and motion perception, and the past reports of acute perceptual disruption due to online TMS (Beynel et al., 2019). This was expected to interact with stimulus intensities such that higher intensities are hypothesized to induce greater behavioral effects. We observed that TMS stimulation applied at the N2-Onset led to behavioral facilitation in motion discrimination relative to Pre-Onset stimulation. However, this effect interacted with stimulation intensity revealing greater facilitation of motion discrimination accuracy at the lowest stimulation intensity of 80% RMT. Furthermore, VEP amplitudes significantly differed for the P3 component, with lower amplitudes in the 80% intensity condition for the Pre-Onset condition and higher amplitudes in the 120% intensity condition for the N2-Onset condition. These results suggest that timing and intensity interact with the profiles of perceptual and electrophysiological responses to near threshold motion stimuli with the additional indication that behavioral facilitation is being promoted by lower intensity stimulation.

4.1. TMS effects on motion perception

Past studies have reported a wide variety of behavioral effects that result from single or paired pulse TMS over a range of factors, such as timing, intensity, and the ongoing activation state of the stimulated region (de Graaf et al., 2014; Romei et al., 2016; Sandrini et al., 2011; Wagner et al., 2007). Although single-pulse TMS has mainly been shown to be disruptive (Abrahamyan et al., 2015; Amassian et al., 1989; Beckers and Zeki, 1995; Desmond et al., 2005), it has been reported that facilitation can be achieved with the right combination of stimulation timing, intensity and background brain state (Abrahamyan et al., 2011; Abrahamyan et al., 2015; Silvanto et al., 2017; Silvanto et al., 2018). For example, enhanced target detection has been found after stimulating the visual cortex with low intensity single pulse TMS delivered 100 and 120 ms after stimulus onset (Abrahamyan et al., 2011, 2015). In these cases, it was proposed that the summation of ongoing neural responses and the excitation induced by the lower intensity TMS pulse resulted in enhanced processing and behavioral facilitation. This explanation is similar to the stochastic resonance account (Schwarzkopf et al., 2011; Stocks, 2000) which proposes that the strength of a stimulus can be improved by externally enhancing the ongoing neural activity. That is, a single pulse of TMS, delivered at low intensity, leads to additional low-amplitude noise to the neural system, boosting information exchange between the neurons in the stimulated cortex (Silvanto et al., 2017).

While such a model may explain the observed effects, other factors may also contribute to facilitation or inhibition in such contexts (Cattaneo and Silvanto, 2008). For example, adaptation that may result from repeated presentations of a stimulus has been shown to influence TMS effects demonstrating that TMS can reverse the influence of adaptation on target detection (Silvanto et al., 2007). Similarly, TMS applied during the delay between a visual priming stimulus and a target stimulus also leads to selective modulation of the target to reduce the priming effect, which demonstrates that attributes encoded by less active neural populations are preferentially facilitated by TMS (Cattaneo and Silvanto, 2008). Finally, as proposed in other studies showing modulatory effects of TMS to V5 in the N2 latency range (Laycock et al., 2007; Sack et al., 2006), which in turn may reflect feedforward/feedback processing between the striate and extrastriate cortices, or possibly the relative contribution of magnocellular and parvocellular inputs to the system. The current findings build on these theorized mechanisms to provide additional insight into state-dependency of TMS effects by describing systematically the influences of stimulation parameters on behavior, most notably that lower intensities can produce greater enhancement effects.

4.2. TMS effects on motion VEPs

The combination of TMS and EEG is a powerful tool for investigating cortical mechanisms and networks with fine temporal precision. Using this technique, we expected to obtain electrophysiological evidence of the interplay between brain activity and TMS conditions. While we did not foresee changes in the electrocortical signature in the “Pre–Onset” condition, we anticipated that due to temporally-precise interruption in motion processing caused by TMS at the onset of the N2 component, modifications in the P3 component would be observable. In particular, it was expected that reductions in the P3 amplitude would result from interruption to perceptual decision making (Luber et al., 2020), leading to increased cognitive load and reduced processing capacity, which has previously been tied to P3 amplitudes (Kok, 2001). Our results showed that the mean activity of the P3 component in the CP ROI produced significant differences between intensities in both timing conditions. In general, high intensity single pulse TMS evoked higher mean activity values for the P3 component than pulses at low intensities. In the Pre-Onset 80% condition, values were significantly smaller than for the higher intensity TMS conditions, while values were significantly higher for the 120% condition at N2-Onset when compared to the lower intensity conditions, but not to vertex-120%. The mean activity increase, however, did not correlate with the magnitude of behavioral effects across participants. While N2 amplitudes generally scaled monotonically with higher stimulation intensities, they did not differ significantly across conditions or correlate with behavioral effects.

In interpreting these effects, it is possible that the EEG activity measured here may have been impacted indirectly by brain stimulation. Namely, despite the presence of both a no-stimulation control and a vertex control, the lack of a somatosensory-matched sham condition is a limitation of this study and the observed intensity effects may be attributed to (multi)sensory evoked activity and not necessarily the result of neural changes due to the induced magnetic field (Casarotto et al., 2010; Conde et al., 2019). As discussed by others (Siebner et al., 2019), an important contributor to the TMS-EEG response is the prominent auditory evoked potential associated with the clicking sound produced by TMS. This auditory response is introduced by a combination of bone-conduction and air conducted sound reaching the cochlea and activating central and parieto-temporal regions bilaterally to produce a prominent N1–P2 complex (Lioumis et al., 2009). Reducing sound levels and distancing the coil from the head have been shown to reduce the N1–P2 complex amplitude (Kähkönen, Wilenius, Komssi and

Ilmoniemi, 2004; Nikouline et al., 1999; ter Braack et al., 2015), and while earplugs and foam insulation were used to mitigate sound here, it is possible that these measures were not sufficient to suppress the auditory response. Thus, future studies should strive to use a more sensitive somatosensory-matched sham control condition to better isolate TMS effects. An alternative explanation for the amplitude scaling of the P3 response, not relevant for the N2 component, may pertain to attentional capture which is greater for higher stimulation intensity. As noted, the P3 response is strongly associated with attentional processes (Kuba et al., 1998; Kubová et al., 2002) and therefore, a plausible explanation of the effects may arise from uncontrolled attentional allocation.

An additional, related observation in this study was that during the Pre-Onset condition we found the presence of an early component at a latency roughly equivalent to the P1. This response was not present in the 0% intensity condition, nor during the early stages of the EEG response in the N2-Onset condition, increasing the possibility that this response may have been driven entirely by the TMS pulse and is not associated with the visual stimulus or the interaction between visual and magnetic stimulation. Further control sessions, performed with a subset of seven participants, who received TMS without visual stimulation (see Supplementary Figure 1) also produced robust EEG responses in the P1 range, further supporting this assumption that this response is driven by the TMS pulse rather than interactions with evoked visual responses. As noted above, such findings need to be considered in the context of multisensory stimulation as well as associated artifacts in the TMS response (Bonato et al., 2006; S. Kähkönen, Komssi, Wilenius and Ilmoniemi, 2005; Lioumis et al., 2009).

4.3. Limitations, future directions and conclusions

While the present study offered a systematic view of the interaction between TMS intensity and relative timing on both behavior and electrophysiological brain responses, there are a number of limitations that should be considered and improved upon in future studies. As noted in the section above, one such limitation is the possible presence of multisensory stimulation confounds that should be better controlled using somatosensory-matched electrical stimulation in future studies. Another point to consider is that it was intended that the motion stimulus would be defined as the dot coherence at 75% accuracy. As observed in Table 1, many of the participants did not reach this criterion in the dose-finding session and therefore 100% coherence was used for these individuals. Despite this, all participants showed largely monotonic accuracy versus coherence functions, as illustrated in Fig. 2A. A possible reason that participants didn't reach the 75% criteria is that the duration of the motion stimulus was intentionally selected to be very short (75 ms) so that spTMS would not be overpowered by a long bottom-up stimulus that could outlast the potential effects of stimulation. This limitation should therefore be considered in light of the tradeoff between motion stimulus salience and the robustness of the stimulation.

Another consideration is the approach used to define stimulation intensity, which was delivered relative to resting motor threshold. While RMT intensity scaling is principled, objective, and widely used, the dosing is based upon motor system responsiveness and not visual system responsiveness. Therefore, the current findings need to be considered in light of previous research showing that MEPs can be elicited at intensities below RMT, which have distinct recruitment (i.e. input-output) curves for inhibitory processes that typically elicit lower threshold than for excitatory processes in motor cortex (Kallioniemi et al., 2014). Moreover, while there is also literature showing that phosphene thresholds are generally higher than motor thresholds (Antal et al., 2004; Boroojerdi et al., 2002; Deblieck et al., 2008), there is also considerable heterogeneity in the ability to elicit phosphenes in individual subjects. Similarly, pilot studies conducted in preparation for this study also resulted in considerable heterogeneity of phosphene responses, and therefore RMT intensity scaling was adopted instead. In light of these challenges, future studies may wish to build on the current dose–response functions to include intensity scaling based on visual responsiveness. Lastly, it is worth noting that there is an important movement towards more powerful sample sizes in TMS studies. While the current sample of 14 individuals who completed all study activities is larger than the average sample size of 11 reported in a recent meta-analysis of online TMS studies (Beynel et al., 2019), future studies should strive for even larger sample sizes.

Funding

Funding was provided by the National Institute of Mental Health of the National Institutes of Health under BRAIN Initiative Award, RF1MH114253. The content is solely the responsibility of the authors and does not necessarily represent the official views of the National Institutes of Health.

CRediT authorship contribution statement

Olga Lucia Gamboa Arana: Conceptualization, Formal analysis, Investigation, Methodology, Writing - original draft, Writing - review & editing. **Hannah Palmer:** Data curation, Investigation, Writing - original draft, Writing - review & editing. **Moritz Dannhauer:** Conceptualization, Formal analysis, Methodology. **Connor Hile:** Data curation, Investigation. **Sicong Liu:** Formal analysis, Writing - review & editing. **Rena Hamdan:** Methodology. **Alexandra Brito:** Data curation, Investigation, Writing - original draft, Writing - review & editing. **Roberto Cabeza:** Conceptualization, Funding acquisition, Writing - review & editing. **Simon W. Davis:** Conceptualization, Funding acquisition, Writing - review & editing. **Angel V. Peterchev:** Conceptualization, Funding acquisition, Methodology, Writing - review & editing. **Marc A. Sommer:** Conceptualization, Funding acquisition, Writing - review & editing. **Lawrence G. Appelbaum:** Conceptualization, Formal analysis, Funding acquisition, Methodology, Project administration, Resources, Supervision, Writing - original draft, Writing - review & editing.

Acknowledgments:

The authors would like to thank Zachary Abzug, Lysianne Beynel, Tracy D'Arbeloff, Erik A. Wing, and Rachel Donaldson, who helped develop the behavioral task and Lari Koponen who help with the concurrent TMS-EEG protocols used in this research. The authors would also like to thank all of the individuals who participated in this research.

Appendix A. Supplementary data

Supplementary data to this article can be found online at https://doi.org/10.1016/j.neuropsychologia.2020.107581.

References

Abrahamyan, A., Clifford, C.W.G., Arabzadeh, E., Harris, J.A., 2011. Improving visual sensitivity with subthreshold transcranial magnetic stimulation. J. Neurosci. 31 (9), 3290–3294. https://doi.org/10.1523/JNEUROSCI.6256-10.2011.

Abrahamyan, A., Clifford, C.W.G., Arabzadeh, E., Harris, J.A., 2015. Low intensity TMS enhances perception of visual stimuli. Brain Stimulation 8 (6), 1175–1182. https://doi.org/10.1016/j.brs.2015.06.012.

Amassian, V.E., Cracco, R.Q., Maccabee, P.J., Cracco, J.B., Rudell, A., Eberle, L., 1989. Suppression of visual perception by magnetic coil stimulation of human occipital cortex. Electroencephalogr. Clin. Neurophysiol.Evoked Potentials 74 (6), 458–462. https://doi.org/10.1016/0168-5597(89)90036-1.

Antal, A., Nitsche, M.A., Kincses, T.Z., Lampe, C., Paulus, W., 2004. No correlation between moving phosphene and motor thresholds: a transcranial magnetic stimulation study. Neuroreport 15 (2), 297–302. https://doi.org/10.1097/00001756-200402090-00017.

Bach, M., Ullrich, D., 1997. Contrast dependency of motion-onset and pattern-reversal VEPs: interaction of stimulus type, recording site and response component. Vis. Res. 37 (13), 1845–1849. https://doi.org/10.1016/S0042-6989(96)00317-3.

Beckers, G., Homberg, V., 1992. Cerebral visual motion blindness: transitory akinetopsia induced by transcranial magnetic stimulation of human area V5. Proc. Biol. Sci. 249 (1325), 173–178. https://doi.org/10.1098/rspb.1992.0100.
Beckers, G., Zeki, S., 1995. The consequences of inactivating areas V1 and V5 on visual motion perception. Brain 118 (1), 49–60. https://doi.org/10.1093/brain/118.1.49.
Beynel, L., Appelbaum, L.G., Luber, B., Crowell, C.A., Hilbig, S.A., Lim, W., et al., 2019. Effects of online repetitive transcranial magnetic stimulation (rTMS) on cognitive processing: a meta-analysis and recommendations for future studies. Neurosci. Biobehav. Rev. https://doi.org/10.1016/j.neubiorev.2019.08.018.
Bonato, C., Miniussi, C., Rossini, P.M., 2006. Transcranial magnetic stimulation and cortical evoked potentials: a TMS/EEG co-registration study. Clin. Neurophysiol. 117 (8), 1699–1707. https://doi.org/10.1016/j.clinph.2006.05.006.
Borckardt, J.J., Nahas, Z., Koola, J., George, M.S., 2006. Estimating resting motor thresholds in transcranial magnetic stimulation research and practice: a computer simulation evaluation of best methods. J. ECT 22 (3), 169–175. https://doi.org/10.1097/01.yct.0000235923.52741.72.
Boroojerdi, B., Meister, I.G., Foltys, H., Sparing, R., Cohen, L.G., Töpper, R., 2002. Visual and motor cortex excitability: a transcranial magnetic stimulation study. Clin. Neurophysiol. 113 (9), 1501–1504. https://doi.org/10.1016/S1388-2457(02)00198-0.
Bosco, G., Carrozzo, M., Lacquaniti, F., 2008. Contributions of the human temporoparietal junction and MT/V5+ to the timing of interception revealed by transcranial magnetic stimulation. J. Neurosci. 28 (46), 12071–12084. https://doi.org/10.1523/JNEUROSCI.2869-08.2008.
Brainard, D.H., 1997. The psychophysics toolbox. Spatial Vis. 10 (4), 433–436. https://doi.org/10.1163/156856897X00357.
Campana, G., Cowey, A., Walsh, V., 2002. Priming of motion direction and area V5/MT: a test of perceptual memory. Cerebr. Cortex 12 (6), 663–669. https://doi.org/10.1093/cercor/12.6.663.
Casarotto, S., Lauro, L.J.R., Bellina, V., Casali, A.G., Rosanova, M., Pigorini, A., et al., 2010. EEG responses to TMS are sensitive to changes in the perturbation parameters and repeatable over time. PloS One 5 (4), e10281. https://doi.org/10.1371/journal.pone.0010281.
Cattaneo, Z., Silvanto, J., 2008. Investigating visual motion perception using the transcranial magnetic stimulation-adaptation paradigm. Neuroreport 19 (14), 1423–1427. https://doi.org/10.1097/WNR.0b013e32830e0025.
Clark, K., Appelbaum, L.G., van den Berg, B., Mitroff, S.R., Woldorff, M.G., 2015. Improvement in visual search with practice: mapping learning-related changes in neurocognitive stages of processing. J. Neurosci. 35 (13), 5351–5359. https://doi.org/10.1523/JNEUROSCI.1152-14.2015.
Conde, V., Tomasevic, L., Akopian, I., Stanek, K., Saturnino, G.B., Thielscher, A., et al., 2019. The non-transcranial TMS-evoked potential is an inherent source of ambiguity in TMS-EEG studies. Neuroimage 185, 300–312. https://doi.org/10.1016/j.neuroimage.2018.10.052.
Conforto, A.B., Z'Graggen, W.J., Kohl, A.S., Rösler, K.M., Kaelin-Lang, A., 2004. Impact of coil position and electrophysiological monitoring on determination of motor thresholds to transcranial magnetic stimulation. Clin. Neurophysiol. 115 (4), 812–819. https://doi.org/10.1016/j.clinph.2003.11.010.
D'Alfonso, A.A.L., Van Honk, J., Schutter, D.J.L.G., Caffé, A.R., Postma, A., De Haan, E.H.F., 2002. Spatial and temporal characteristics of visual motion perception involving V5 visual cortex. Neurol. Res. 24 (3), 266–270. https://doi.org/10.1179/016164102101199891.
de Graaf, T.A., Koivisto, M., Jacobs, C., Sack, A.T., 2014. The chronometry of visual perception: review of occipital TMS masking studies. Neurosci. Biobehav. Rev. 45, 295–304. https://doi.org/10.1016/j.neubiorev.2014.06.017.
Deblieck, C., Thompson, B., Iacoboni, M., Wu, A.D., 2008. Correlation between motor and phosphene thresholds: a transcranial magnetic stimulation study. Hum. Brain Mapp. 29 (6) https://doi.org/10.1002/hbm.20427.
Desmond, J.E., Chen, S.H.A., Shieh, P.B., 2005. Cerebellar transcranial magnetic stimulation impairs verbal working memory. Ann. Neurol. 58 (4), 553–560. https://doi.org/10.1002/ana.20604.
Duncan-Johnson, C.C., Donchin, E., 1982. The P300 component of the event-related brain potential as an index of information processing. Biol. Psychol. 14 (1–2), 1–52. https://doi.org/10.1016/0301-0511(82)90016-3.
Gamboa, O., Brito, A., Abzug, Z., D'Arbeloff, T., Beynel, L., Wing, E.A., et al., 2020. Application of long-interval paired-pulse transcranial magnetic stimulation to motionsensitive visual cortex does not lead to changes in motion perception. Neurosci. Lett. 135022. https://doi.org/10.1016/j.neulet.2020.135022.
Grasso, P.A., Làdavas, E., Bertini, C., Caltabiano, S., Thut, G., Morand, S., 2018. Decoupling of early V5 motion processing from visual awareness: a matter of velocity as revealed by transcranial magnetic stimulation. J. Cognit. Neurosci. 30 (10), 1517–1531. https://doi.org/10.1162/jocn_a_01298.
Hallett, M., Di Iorio, R., Rossini, P.M., Park, J.E., Chen, R., Celnik, P., et al., 2017. Contribution of transcranial magnetic stimulation to assessment of brain connectivity and networks. Clin. Neurophysiol. 128 (11), 2125–2139. https://doi.org/10.1016/j.clinph.2017.08.007.
Kähkönen, S., Komssi, S., Wilenius, J., Ilmoniemi, R.J., 2005. Prefrontal transcranial magnetic stimulation produces intensity-dependent EEG responses in humans. Neuroimage 24 (4), 955–960. https://doi.org/10.1016/j.neuroimage.2004.09.048.
Kähkönen, Seppo, Wilenius, J., Komssi, S., Ilmoniemi, R.J., 2004. Distinct differences in cortical reactivity of motor and prefrontal cortices to magnetic stimulation. Clin. Neurophysiol. 115 (3), 583–588. https://doi.org/10.1016/j.clinph.2003.10.032.
Kallioniemi, E., Säisänen, L., Könönen, M., Awiszus, F., Julkunen, P., 2014. On the estimation of silent period thresholds in transcranial magnetic stimulation. Clin. Neurophysiol. 125 (11), 2247–2252. https://doi.org/10.1016/j.clinph.2014.03.012.
Kok, A., 2001. On the utility of P3 amplitude as a measure of processing capacity. Psychophysiology 38 (3), 557–577. https://doi.org/10.1017/S0048577201990559.
Kuba, M., Kremláček, J., Kubová, Z., 1998. Cognitive evoked potentials related to visual perception of motion in human subjects. Physiol. Res. 47 (4), 265–270.
Kuba, M., Kubová, Z., Kremláček, J., Langrová, J., 2007. Motion-onset VEPs: characteristics, methods, and diagnostic use. Vis. Res. 47 (2), 189–202. https://doi.org/10.1016/j.visres.2006.09.020.
Kubová, Z., Kremláček, J., Szanyi, J., Chlubnová, J., Kuba, M., 2002. Visual event-related potentials to moving stimuli: normative data. Physiol. Res. 51 (2), 199–204.
Laycock, R., Crewther, D.P., Fitzgerald, P.B., Crewther, S.G., 2007. Evidence for fast signals and later processing in human V1/V2 and V5/MT+: a TMS study of motion perception. J. Neurophysiol. 98 (3), 1253–1262. https://doi.org/10.1152/jn.00416.2007.
Lioumis, P., Kičić, D., Savolainen, P., Mäkelä, J.P., Kähkönen, S., 2009. Reproducibility of TMS—evoked EEG responses. Hum. Brain Mapp. 30 (4), 1387–1396. https://doi.org/10.1002/hbm.20608.
Luber, B., Jangraw, D.C., Appelbaum, G., Harrison, A., Hilbig, S., Beynel, L., et al., 2020. Using transcranial magnetic stimulation to test a network model of perceptual decision making in the human brain. Front. Hum. Neurosci. 14 (4) https://doi.org/10.3389/fnhum.2020.00004.
Luck, S.J., 2014. An Introduction to the Event-Related Potential Technique, second ed. https://doi.org/10.1118/1.4736938
Luck, S.J., Hillyard, S.A., 1990. Electrophysiological evidence for parallel and serial processing during visual search. Percept. Psychophys. 48 (6), 603–617. https://doi.org/10.3758/BF03211606.
Martin, T., Huxlin, K.R., Kavcic, V., 2010. Motion-onset visual evoked potentials predict performance during a global direction discrimination task. Neuropsychologia 48 (12), 3563–3572. https://doi.org/10.1016/j.neuropsychologia.2010.08.005.
Mather, G., Battaglini, L., Campana, G., 2016. TMS reveals flexible use of form and motion cues in biological motion perception. Neuropsychologia 84, 193–197. https://doi.org/10.1016/j.neuropsychologia.2016.02.015.
Matthews, N., Luber, B., Qian, N., Lisanby, S.H., 2001. Transcranial magnetic stimulation differentially affects speed and direction judgments. Exp. Brain Res. 140 (4), 397–406. https://doi.org/10.1007/s002210100837.
Nikouline, V., Ruohonen, J., Ilmoniemi, R.J., 1999. The role of the coil click in TMS assessed with simultaneous EEG. Clin. Neurophysiol. 110 (8), 1325–1328. https://doi.org/10.1016/S1388-2457(99)00070-X.
Pascual-Leone, A., Dang, N., Cohen, L.G., Brasil-Neto, J.P., Cammarota, A., Hallett, M., 1995. Modulation of muscle responses evoked by transcranial magnetic stimulation during the acquisition of new fine motor skills. J. Neurophysiol. 74 (3), 1037–1045. https://doi.org/10.1152/jn.1995.74.3.1037.
Pascual-Leone, A., Walsh, V., 2001. Fast backprojections from the motion to the primary visual area necessary for visual awareness. Science 292 (5516), 510–512. https://doi.org/10.1126/science.1057099.
Pazo-Álvarez, P., Amenedo, E., Lorenzo-López, L., Cadaveira, F., 2004. Effects of stimulus location on automatic detection of changes in motion direction in the human brain. Neurosci. Lett. 371 (2–3), 111–116. https://doi.org/10.1016/j.neulet.2004.08.073.
Rogasch, N.C., Thomson, R.H., Farzan, F., Fitzgibbon, B.M., Bailey, N.W., Hernandez-Pavon, J.C., et al., 2014. Removing artefacts from TMS-EEG recordings using independent component analysis: importance for assessing prefrontal and motor cortex network properties. Neuroimage 101, 425–439. https://doi.org/10.1016/j.neuroimage.2014.07.037.
Romei, V., Thut, G., Silvanto, J., 2016. Information-based approaches of noninvasive transcranial brain stimulation. Trends Neurosci. 39 (11), 782–795. https://doi.org/10.1016/j.tins.2016.09.001.
Rossi, S., Hallett, M., Rossini, P.M., Pascual-Leone, A., Avanzini, G., Bestmann, S., et al., 2009. Safety, ethical considerations, and application guidelines for the use of transcranial magnetic stimulation in clinical practice and research. Clin. Neurophysiol. 120 (12), 2008–2039. https://doi.org/10.1016/j.clinph.2009.08.016.
Ruddy, K.L., Woolley, D.G., Mantini, D., Balsters, J.H., Enz, N., Wenderoth, N., 2018. Improving the quality of combined EEG-TMS neural recordings: introducing the coil spacer. J. Neurosci. Methods 294, 34–39. https://doi.org/10.1016/j.jneumeth.2017.11.001.
Saatlou, F.H., Rogasch, N.C., McNair, N.A., Biabani, M., Pillen, S.D., Marshall, T.R., Bergmann, T.O., 2018. MAGIC: an open-source MATLAB toolbox for external control of transcranial magnetic stimulation devices. Brain Stimulation 11 (5), 1189–1191. https://doi.org/10.1016/j.brs.2018.05.015.
Sack, A.T., Kohler, A., Linden, D.E.J., Goebel, R., Muckli, L., 2006. The temporal characteristics of motion processing in hMT/V5+: combining fMRI and neuronavigated TMS. Neuroimage 29 (4), 1326–1335. https://doi.org/10.1016/j.neuroimage.2005.08.027.
Sandrini, M., Umiltà, C., Rusconi, E., 2011. The use of transcranial magnetic stimulation in cognitive neuroscience: a new synthesis of methodological issues. Neurosci. Biobehav. Rev. 35 (3), 516–536. https://doi.org/10.1016/j.neubiorev.2010.06.005.
Schaeffner, L.F., Welchman, A.E., 2017. Mapping the visual brain areas susceptible to phosphene induction through brain stimulation. Exp. Brain Res. 235 (1), 205–217. https://doi.org/10.1007/s00221-016-4784-4.
Schwarzkopf, D.S., Silvanto, J., Rees, G., 2011. Stochastic resonance effects reveal the neural mechanisms of transcranial magnetic stimulation. J. Neurosci. 31 (9), 3143–3147. https://doi.org/10.1523/JNEUROSCI.4863-10.2011.
Siebner, H.R., Conde, V., Tomasevic, L., Thielscher, A., Bergmann, T.O., 2019. Distilling the essence of TMS-evoked EEG potentials (TEPs): a call for securing mechanistic specificity and experimental rigor. Brain Stimulation 12 (4), 1051–1054. https://doi.org/10.1016/j.brs.2019.03.076.

Silvanto, J., Bona, S., Cattaneo, Z., 2017. Initial activation state, stimulation intensity and timing of stimulation interact in producing behavioral effects of TMS. Neuroscience 363, 134–141. https://doi.org/10.1016/j.neuroscience.2017.09.002.

Silvanto, J., Bona, S., Marelli, M., Cattaneo, Z., 2018. On the mechanisms of Transcranial Magnetic Stimulation (TMS): how brain state and baseline performance level determine behavioral effects of TMS. Front. Psychol. 9, 741. https://doi.org/10.3389/fpsyg.2018.00741.

Silvanto, J., Lavie, N., Walsh, V., 2005. Double dissociation of V1 and V5/MT activity in visual awareness. Cerebr. Cortex 15 (11), 1736–1741.

Silvanto, J., Muggleton, N.G., Cowey, A., Walsh, V., 2007. Neural adaptation reveals state-dependent effects of transcranial magnetic stimulation. Eur. J. Neurosci. 25 (6), 1874–1881. https://doi.org/10.1111/j.1460-9568.2007.05440.x.

Stocks, N.G., 2000. Suprathreshold stochastic resonance in multilevel threshold systems. Phys. Rev. Lett. 84 (11), 2310–2313. https://doi.org/10.1103/PhysRevLett.84.2310.

ter Braack, E.M., de Vos, C.C., van Putten, M.J.A.M., 2015. Masking the auditory evoked potential in TMS–EEG: a comparison of various methods. Brain Topogr. 28 (3), 520–528. https://doi.org/10.1007/s10548-013-0312-z.

Vetter, P., Grosbras, M.H., Muckli, L., 2015. TMS over V5 disrupts motion prediction. Cerebr. Cortex 25 (4), 1052–1059. https://doi.org/10.1093/cercor/bht297.

Wagner, T., Valero-Cabre, A., Pascual-Leone, A., 2007. Noninvasive human brain stimulation. Annu. Rev. Biomed. Eng. 9, 527–565. https://doi.org/10.1146/annurev.bioeng.9.061206.133100.